# Optimal Configuration of An Annular Sector Duct Filled With Porous Media

Research Article

Hafsa Hareem* and Mazhar Iqbal

*School of Natural Sciences, National University of Sciences and Technology, H-12 Islamabad, Pakistan*
**\*Corresponding author:** mazhar.iqbal@sns.nust.edu.pk

**Abstract.** In the current study, optimal configuration for finned annulus, filled with porous media, have been investigated to maximize the convective heat transfer and minimize the friction effect subject to constant heat flux boundary conditions. *Genetic Algorithm* (GA) has been employed to find out the optimal geometry out of vast choices of geometrical parameters; ratio of radii of the inner to outer pipe and sector angle of channel. *Finite Difference Method* (FDM) is applied to solve the governing mathematical model. Chilton-Colburn's $j$ factor is employed as the objective function and numerical solutions of the momentum and energy equations are used as function values to the optimizer. The results indicate that for a fixed Prandtl number ($Pr$) the optimal geometry transforms with the variation in permeability of the porous media which is in line with the physics of the problem.

**Keywords.** Optimal configuration; Porous media; Annulus sector duct; Genetic algorithm; $j$ factor

**MSC.** 35J15; 65N22; 76S99

## 1. Introduction

Optimization is an emerging technique employed in the field of *Computational Fluid Dynamics* (CFD) for finding the best results for numerical simulation in the various disciplines of applied sciences and engineering problems affiliated with fluid flow and heat transfer phenomena. In

the field of applied sciences and engineering, optimization is usually leads to the minimization or maximization of objective function. It is more effective and efficient method in the right direction after denying the old hit and trial methods. It has helped to reduce cost and effort for the expensive experiments held for construction and maturation of fresh products. There are a variety of methods available for the optimization of ones problem which can be easily executed on a computer. Optimization can be categorized into uni-disciplinary and multi-disciplinary based on the kind of results that are needed. As restraints are applied on the objective function of optimization, it is termed as constrained optimization, otherwise it is termed as unconstrained optimization. Optimization techniques that are uni-disciplinary are divided into evolutionary algorithms, gradient based algorithms, hybrid algorithms and simulated annealing algorithms. Multi-disciplinary multi-level optimization techniques consist of *Concurrent Subspace Optimization* (CSSO), *Collaborative Optimization* (CO), *Analytical Target Cascading* (ATC) and *Bi-Level Integrated System Synthesis* (BLISS). Genetic algorithm is an emerging technique in the field of optimization of complex multi-variable real world problems. GA is a category of evolutionary algorithms which is based on the mechanics of natural selection and evolution of species. This study employs genetic algorithm for finding the optimum point for heat transfer and friction effect.

Fluid flow and heat transfer have always been an area of interest for scientists hence a lot of research has been conducted in the different areas of this field. Also, extended surfaces have been a significant technique used to improve the heat transfer rate between fundamental surfaces and the medium surrounding it. Fins are the most popular extended surfaces widely used in the fields of petroleum manufacturing, electronics, chemical factory, power plants, nuclear processes, aerodynamics etc. Even though fins are quite useful in increasing heat transfer rate as they provide more surface area for heat transfer however they posses a few draw backs of increasing friction, weight, cost etc. Hence optimization of duct and fin configuration has become an intriguing sphere of study. In the current research, we have optimized the radius of concentric pipes and number of fins used to raise the heat transfer rate and drop the friction effect for two concentric pipes which have longitudinal fins, joined within the annulus between the internal and external pipe.

Liu [20] studied that duct geometry has great impact on bifurcation structures, heat transfer enhancement potential and flow stability of forced convection. It is concluded that when friction of flow experiences a minor boost, a noteworthy raise in heat transfer potential is observed. Kurtbas and Celik [17] experimentally investigated mixed convection heat transfer of a fluid flowing through a horizontal rectangular channel. It was concluded that the average Nusselt number experiences a rapid upsurge that is proportional to the pore density and the local Nusselt number rises quickly regarding a analyst value of Reynolds number. Hooman *et al.* [8] analyzed the properties of first and second law of thermodynamics for fully developed convection heat transfer in a porous saturated duct having a rectangular cross section. It was concluded that heat transfer rate is best, when porous media shape parameter is less than 10 and the sides

of the duct along the width are heated while others are insulated. Considering when porous media shape parameter is greater than 10, the best results are obtained when only one side of duct is insulated.

Nobari and Mehrabani [22] numerically discussed flow and heat transfer carried out in curved shaped eccentric annuli. It is observed that when dean number is large, rate of heat transfer can be escalated for curved eccentric annuli. This contrasts with straight annuli behavior. The amplification of rate of heat transfer in eccentric curved annuli, for large dean number relies on curvature ratio and eccentricity of annulus. Li *et al.* [18] employed mixing length theory in annular sector ducts to simulate the fully developed flow that is turbulent in nature. The study showed that the friction factor, gathered from the turbulence models does not coincide with test data and mixing length theory is best suited for heat transfer through fully developed flow. Zaim and Nassab [27] numerically analyzed convective heat transfer through water. Inlet fluid temperature governs the Nusselt number and when the temperature advances to pseudo-critical level Nusselt number escalates.

Lin *et al.* [19] numerically studied developing laminar flow and heat transfer in annular sector ducts. It was concluded that both entrance lengths, hydrodynamic and thermal, experience a decreases when the sector angle along with the ratio of diameters of inner and outer pipe expand. Also, the development of hydrodynamic boundary layer falls short to that of thermal boundary layer. Adegun *et al.* [1] numerically analyzed forced convection heat transfer in finned elliptical ducts and the influence that Reynolds number, Prandtl number, aspect ratio, fin heights, number of fins and orientations of the duct has on the heat transfer coefficient, history of temperature and velocity vector. Kaviany [16] studied laminar fluid flow in a porous media contained between two parallel plates. The plates are kept at a constant and equal pressure. The study concluded that in case of a fully developed field, the Nusselt number increases with the rise in shape parameter of porous media. The excess pressure drop has opposite effect than that of Nusselt number, it decreases with the increase in the value of shape parameter. Zeitoun and Hegazy [28] numerically investigated the heat transfer rate for laminar flow through pipes with fins of different height attached in it. The wall temperature is spread uniformly. It was concluded that when pipes are taken to be internally finned then fin height has a great impact on the flow and heat transfer characteristics. Ishaq *et al.* [15] studied laminar forced convective heat transfer when the flow is assumed to be fully developed and the fluid is moving through a finned double pipe annulus. It was observed that when fins of various heights are activated in two groups, the flow and thermal attributes can be improved by adjusting the velocity and temperature distribution. Sung *et al.* [25] numerically analyzed forced convection heat transfer and fluid flow through a channel which is partially filled with porous media. The results indicate that as the thickness of porous substrate increases or Darcy number decreases, the rate of fluid flow experiences an upsurge. While keeping the Darcy number constant, when the ratio of thermal conductivities increase, the heat transfer rate experiences an upsurge. The practicality of using porous media to increase heat transfer is also analyzed.

Optimization of heat transfer in a double tube with fins attached in it was carried out by Colle and Maliska [3] where the flow was considered to be laminar. They also formed an association between the Reynolds number, friction factor, height, fin radius and the number of fins. Genetic algorithm was used for the optimization of fin configuration carried out by Fabbri [5] where the temperature is distributed in two dimensions. The study was conducted to investigate the fin thickness for which fin effectiveness is maximum. Iqbal *et al.* [14] conferred on the optimization of fin shape adhered with the exterior of an inner pipe about a double pipe geometry. The optimization of fin shape is highly reliant on the ratio of radii, number of fins, control points and characteristic length. Iqbal *et al.* [11] took up the optimization of a double pipe with trapezoidal fins attached with the inner pipe. The maximum optimal value of Nusselt number has tremendous inclination upon the measurement of internal pipe. The optimum number of fins is directly proportional to the radius of inner pipe. For an abundant fin number the optimum value can be actualized for higher fins. The dependence of Nusselt number on measure of internal pipe amplifies with the amount of fins employed. Iqbal *et al.* [12] optimized an annulus with parabolic fins for convective heat transfer rate. The optimal configuration relies on both the hydraulic and equivalent diameter. The optimal configuration comparison of parabolic fins with triangular and trapezoidal fins, indicates that no fin shape is perfect, according to every criteria. Iqbal *et al.* [13] optimized the configuration of longitudinal fins adhered to the outer surface of the inner pipe in a concentric pipe geometry. It is concluded that the optimal fin shape is dependent on the number of fins and their characteristic length, conduction properties of the heated surfaces and number of control points. The optimal fin shape that maximizes the conjugate heat transfer coefficient is wavy and the optimal fin configuration improves the Nusselt number till 289%.

Iqbal and Afaq [10] numerically analyzed fluid flow and heat transfer through an annular sector duct filled with porous media which indicated that an optimum geometry exists where we can observe heat transfer rate at its peak. Also as far as we know no research has been conducted to find the optimum value of fluid flow and heat transfer through porous media filled inside an annular sector duct. Optimization holds great importance in the field of computational fluid mechanics. We optimized fluid flow and heat transfer through a finned annular sector duct filled with porous media by employing genetic algorithm as our optimization technique. Results are evaluated for the product of fanning friction factor to Reynold's number (*fRe*) and Nusselt number (*Nu*). It was concluded that with the decrease in permeability, the optimum values of *fRe* and *Nu* both exhibit an increase. Their response to the alterations in ratio of radii, permeability and number of fins will be analyzed. Tabular and graphical illustrations are utilized to show the results.

## 2. Problem Formulation

For the current research we have considered a steady, laminar, thermally and hydro-dynamically fully developed flow. The fluid is taken to be incompressible, viscous and Newtonian flowing

through an annular sector duct packed with Darcy-Brinkman's porous media. Vertical fins are inserted in the duct's annulus between the external and internal pipe (as presented in Figure 2.1a). The radius of internal and external pipe is considered to be $r_i$ and $r_o$, respectively, and the sector angle that is the angle between two consecutive fins is taken as $2\alpha$. Geometrical symmetry can be observed in Figure 2.1a, on account of that the computational domain is considered as half of the region that is contained between successive fins (seen through Figure 2.1b). Hence computational sector angle is taken as $\alpha$ and sector length is represented by $r_o - r_i$. Forced convection is carried out by moving heated fluid through inner pipe whereas cold fluid through outer pipe synchronously. The outer pipe's external surface is insulated to prevent heat loss across this surface. Hence the only heat transferring surfaces are the inner pipe and longitudinal fins.

All body forces, viscous dissipation and heat conduction in axial direction is taken to be negligible. The modeling of the problem undergoes constant heat flux boundary conditions, commonly known as $H_1$ boundary conditions [24]. These boundary conditions are executed on the inner expanse of heat transferring surfaces. Constant pressure gradient is the sole driving force in the axial (z) direction.

The continuity equation in cylindrical polar coordinates can be expressed in the following form:

**Continuity Equation**

$$\frac{\partial \rho}{\partial t} + \frac{\partial (\rho r u)}{r \partial r} + \frac{\partial \rho v}{r \partial \theta} + \frac{\partial \rho w}{\partial z} = 0. \tag{2.1}$$
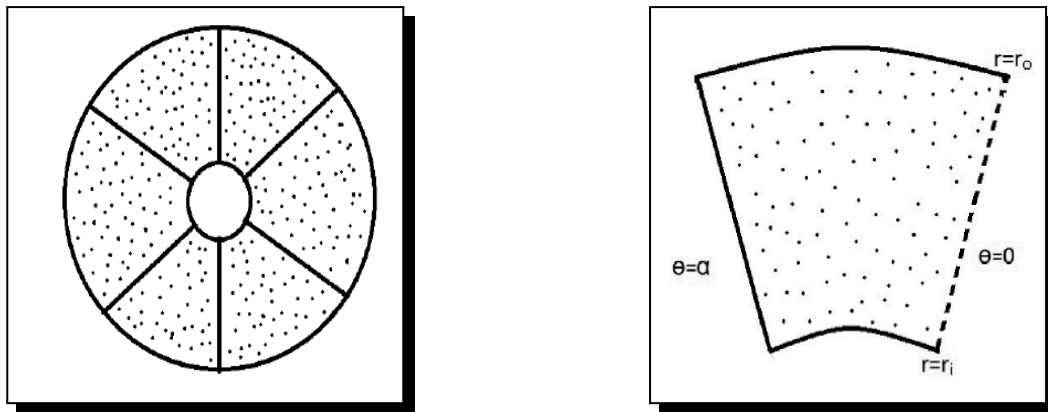


**(a)** Cross-sectional view of concentric pipes      **(b)** Computational domain

**Figure 2.1.** Geometry of duct

## 2.1 Momentum Equation

$$\rho \left( \frac{\partial u}{\partial t} + u \frac{\partial u}{\partial r} + \frac{v}{r} \frac{\partial u}{\partial \theta} + w \frac{\partial u}{\partial z} - \frac{v^2}{r} \right)$$
$$= -\frac{\partial P}{\partial r} + \mu \left[ \frac{\partial}{r \partial r} \left( r \frac{\partial u}{\partial r} \right) \right] + \mu \left( \frac{1}{r^2} \frac{\partial^2 u}{\partial \theta^2} + \frac{\partial^2 u}{\partial z^2} - \frac{u}{r^2} - \frac{2}{r^2} \frac{\partial v}{\partial \theta} - \frac{u}{K} \right) + \rho g_r, \tag{2.2}$$

$$\rho \left( \frac{\partial v}{\partial t} + u \frac{\partial v}{\partial r} + \frac{v}{r} \frac{\partial v}{\partial \theta} + w \frac{\partial v}{\partial z} - \frac{uv}{r} \right)$$

$$= -\frac{1}{r} \frac{\partial P}{\partial \theta} + \mu \left( \frac{\partial}{r \partial r} \left( r \frac{\partial v}{\partial r} \right) \right) + \mu \left( \frac{1}{r^2} \frac{\partial^2 v}{\partial \theta^2} + \frac{\partial^2 v}{\partial z^2} - \frac{v}{r^2} + \frac{2}{r^2} \frac{\partial u}{\partial \theta} - \frac{v}{K} \right) + \rho g_\theta, \tag{2.3}$$

$$\rho \left( \frac{\partial w}{\partial t} + u \frac{\partial w}{\partial r} + \frac{v}{r} \frac{\partial w}{\partial \theta} + w \frac{\partial w}{\partial z} \right) = -\frac{\partial P}{\partial z} + \mu \left( \frac{\partial}{r \partial r} \left( r \frac{\partial w}{\partial r} \right) \right) + \mu \left( \frac{1}{r^2} \frac{\partial^2 w}{\partial \theta^2} + \frac{\partial^2 w}{\partial z^2} - \frac{w}{K} \right) + \rho g_z. \tag{2.4}$$

In the above equations, $K$ is considered as the permeability of the medium, $\rho$ is density of the medium (fluid), $(u, v, w)$ are the velocity components of the fluid, $\mu$ is the dynamic viscosity and $(g_r, g_\theta, g_z)$ are the components of gravitational effect on the fluid or it can be summed up as the body forces on the fluid. After the application of the geometric conditions and assumptions for this study, the continuity equation is satisfied and momentum equations reduce to

$$\frac{\partial^2 w}{\partial r^2} + \frac{1}{r} \frac{\partial w}{\partial r} + \frac{1}{r^2} \frac{\partial^2 w}{\partial \theta^2} - \frac{w}{K} = \frac{1}{\mu} \frac{\partial P}{\partial z}, \tag{2.5}$$

where the prescribed boundary conditions on reduced momentum equation (2.5) are

$$\text{for } r = r_i, \quad w = 0 \qquad 0 \le \theta \le \alpha \tag{2.6}$$

$$\text{for } r = r_o, \quad w = 0 \qquad 0 \le \theta \le \alpha \tag{2.7}$$

$$\text{for } \theta = 0, \quad \frac{\partial w}{\partial \theta} = 0 \quad r_i \le r \le r_o \tag{2.8}$$

$$\text{for } \theta = \alpha, \quad w = 0 \quad r_i \le r \le r_o \tag{2.9}$$

To make above reduced momentum equation and its boundary equations dimensionless we introduce the following parameters

$$R = \frac{r}{r_o}, \qquad \widetilde{R} = \frac{r_i}{r_o}, \tag{2.10}$$

$$\widehat{w} = -\frac{w}{\frac{1}{\mu} r_o^2 \frac{\partial P}{\partial z}}, \quad \widehat{K} = \frac{K}{r_o^2}. \tag{2.11}$$

Here $\widehat{K}$ is Darcy number. So now with the help of above parameters (2.10) and (2.11), the dimensionless momentum equation can be written as

$$\frac{\partial^2 \widehat{w}}{\partial R^2} + \frac{1}{R} \frac{\partial \widehat{w}}{\partial R} + \frac{1}{R^2} \frac{\partial^2 \widehat{w}}{\partial \theta^2} - \frac{\widehat{w}}{\widehat{K}} = -1. \tag{2.12}$$

The boundary conditions given in equations (2.6)-(2.9) are thus transformed into

$$\text{for } R = \widetilde{R}, \quad \widehat{w} = 0 \qquad 0 \le \theta \le \alpha \tag{2.13}$$

$$\text{for } R = 1, \quad \widehat{w} = 0 \qquad 0 \le \theta \le \alpha \tag{2.14}$$

$$\text{for } \theta = 0, \quad \frac{\partial \widehat{w}}{\partial \theta} = 0 \quad r_i \le r \le r_o \tag{2.15}$$

$$\text{for } \theta = \alpha, \quad \widehat{w} = 0 \quad r_i \le r \le r_o \tag{2.16}$$

## 2.2 Energy Equation

The energy equation can be used to observe the heat transfer through a fluid flow. For cylindrical polar coordinates it can be expressed as

$$\rho c_p \left( \frac{\partial T}{\partial t} + u \frac{\partial T}{\partial r} + \frac{v}{r} \frac{\partial T}{\partial \theta} + w \frac{\partial T}{\partial z} \right) = \kappa \left( \frac{\partial^2 T}{\partial r^2} + \frac{1}{r} \frac{\partial T}{\partial r} + \frac{1}{r^2} \frac{\partial^2 T}{\partial \theta^2} + \frac{\partial^2 T}{\partial z^2} \right), \tag{2.17}$$

where $\rho$ is taken as the density of fluid, $\kappa$ is the thermal conductivity of fluid and $c_p$ as the specific heat capacity. Due to the resections and assumptions taken for this study the energy equation can be reduced to

$$\frac{\partial^2 T}{\partial r^2} + \frac{1}{r}\frac{\partial T}{\partial r} + \frac{1}{r^2}\frac{\partial^2 T}{\partial \theta^2} = \frac{\rho c_p}{\kappa}\left(w\frac{\partial T}{\partial z}\right).$$

(2.18)

The boundary conditions for the governing equation can be expressed as

$$T = T_w(z) \quad \text{at } r = r_i, \quad 0 \le \theta \le \alpha$$

(2.19)

$$\frac{\partial T}{\partial r} = 0 \qquad \text{at } r = r_o, \quad 0 \le \theta \le \alpha$$

(2.20)

$$\frac{\partial T}{\partial \theta} = 0 \qquad \text{at } \theta = 0, \quad r_i \le r \le r_o$$

(2.21)

$$T = T_w(z), \quad \text{at } \theta = \alpha, \quad r_i \le r \le r_o$$

(2.22)

where $T_w$ is taken as the wall temperature that varies axially with the coordinate $z$, for a constant rate of heat throughout the pipe. For a smooth heat transfer the temperature distribution and wall temperature should be different and alter axially. For a temperature field independent of axial coordinate we form a non-dimensional parameter $\tau$, where the flow is taken to be thermally fully developed.

$$\tau = \frac{T - T_W}{\frac{q'}{\kappa}}.$$

(2.23)

Here $q'$ is taken as heat transfer rate per unit length in axial direction of duct. After incorporating $\tau$ into energy equation (2.18) it reduces to (the details of calculation can be seen [10])

$$\frac{\partial^2 T}{\partial r^2} + \frac{1}{r}\frac{\partial T}{\partial r} + \frac{1}{r^2}\frac{\partial^2 T}{\partial \theta^2} = \frac{w}{A_c w_m}\frac{q'}{\kappa}.$$

(2.24)

To make reduced energy equation and its boundary equations dimensionless we introduce the same parameters as given in (2.10) and (2.11). Hence (2.24) in non-dimensional form is expressed as

$$\frac{\partial^2 \tau}{\partial R^2} + \frac{1}{R}\frac{\partial \tau}{\partial R} + \frac{1}{R^2}\frac{\partial^2 \tau}{\partial \theta^2} = \frac{\widehat{w}}{A_c \widehat{w}_m},$$

(2.25)

where $\widehat{w}_m$ represents the non-dimensional mean velocity. The dimensionless parameters transform the boundary conditions (2.19)-(2.22) of energy equation into:

$$\text{at } R = \widetilde{R}, \quad \tau = 0, \qquad 0 \le \theta \le \alpha$$

(2.26)

$$\text{at } \quad R = 1, \quad \frac{\partial \tau}{\partial R} = 0, \quad 0 \le \theta \le \alpha$$

(2.27)

$$\text{at } \quad \theta = 0, \quad \frac{\partial \tau}{\partial \theta} = 0, \quad \widetilde{R} \le R \le 1$$

(2.28)

$$\text{at } \quad \theta = \alpha, \quad \tau = 0, \qquad \widetilde{R} \le R \le 1$$

(2.29)

*Finite Difference Method* (FDM) is employed to discretize the governing equations (2.12) and (2.25) by applying five point stencil. The resulting algebraic equations can be simplified using a numerical technique called *Successive Over Relaxation* (SOR) method.

## 3. Optimization Method

For the current study, we have optimized fluid flow and heat transfer through a finned annulus. The computational domain can be observed in Figure 2.1b, where bound constraints are placed on ratio of radii and number of fins. Genetic Algorithm is being employed for the optimization of our problem. In this section we will study the method for the optimization of our problem i.e. *Genetic Algorithm* (GA) which is probabilistic in nature. The study of this technique will help us to determine its efficiency and other traits for optimizing a problem. We execute this procedure for optimization using mathematical codes in MATLAB. To understand the optimization technique better its general frame-work is discussed below.

### 3.1 Genetic Algorithm

*Genetic Algorithm* (GA) [5, 7] is a global search procedure used to solve both constrained and unconstrained optimization problems. It is inspired from Darwin's theory of evolution. It belongs to the class of *Evolutionary Algorithms* (EA) and applies almost the same technique as EA to optimize the solution by natural selection and survival of the fittest. For each iteration the GA starts with selecting a random initial population from domain. It generates offspring generation by determining the fitness function value of each individual that belongs to the random initial population. Then selection criteria such as roulette wheel selection, tournament selection methods are employed to choose suitable parents based on the fitness value. After the selection of appropriate and fit parent generation offspring are formed either by crossing-over or mutation. Crossing-over keeps the good attributes of parents in offspring hence producing a better generation whereas mutation provides diversity. The offspring then replaces some old parent point in the population hence forming a new generation. The algorithm moves to evaluating the fitness value of each new generation and repeats all steps until stopping criteria is met.

Genetic algorithm is favored for optimization over other procedures due to its accuracy and reliable nature. Because GA works on many points in the domain relative to the objective function so it escapes local maxima and minima and strives for global minima. The objective function does not necessarily need to be in refined form or in specific formula, GA can work directly on domain points and fitness values can be gained with help of experimentation. It can work quite efficiently to solve large scale problem. On the other hand every technique has its short comings some of them are mentioned as:

GA is expensive. Sometimes it can take days to reach the convergence/stopping criteria. Ever now and then premature convergence occurs that disrupts the search of global optimum. It has a high probability to reach global optimum but it is an undirected search due to generation of a random initial population so it cannot always be directed towards optimal solution area.

## 4. Optimization Problem and its Modeling

We have maximized Colburn's *j* factor for ratio of radii and sector angle of channel. Colburn's *j* factor is a non-dimensional quantity which is an analogy that relates heat transfer coefficients, mass transfer coefficients and friction factor. The ratio of radii $\left(\widetilde{R} = \frac{r_i}{r_o}\right)$ and number of fins (*nof*) are bounded to provide us a better understanding of the behavior of objective function.

The significance of this research can be highlighted through Figures 4.2 and 4.1. In Figures 4.2 and 4.1, we demonstrate the effect of $\widetilde{R}$ on *fRe* and *Nu* for a given value of permeability. The sub-figures express a general trend for distinct values of $\widetilde{R}$. Here the value of permeability is kept constant at 0.001 i.e. $\widehat{K} = 0.001$. It is observed in Figure 4.1 that with the increase in *nof*, *fRe* experiences a downward slope. Also with the increase in the value of $\widetilde{R}$ the passage for fluid flow decreases hence the curve that shows the trend of *fRe* starts straightening out, the peak values of graph decreases but a general increase in the value of *fRe* is observed, this happens due to the constriction in space which restricts the motion of fluid hence causing friction effect to increase.

It can be observed that when $\widetilde{R}$ is small, in the beginning *Nu* increases then gradually starts decreasing whereas with the increasing value of $\widetilde{R}$ the trend is reversed. This non-monotonic behavior is an indication of an optimal geometry for which heat transfer rate can be maximized. Hence our aim is to find an optimum solution for which heat transfer rate is maximum whereas friction effect is at its minimum. We can visualize the behavior of *Nu* and *fRe* for a handful of values of $\widetilde{R}$ by taking 0.1 increment between adjacent values of $\widetilde{R}$ through Figures 4.2 and 4.1, which represent the results for only eight values of $\widetilde{R}$ against $\widehat{K} = 0.001$. Now if we take full range of parameters i.e. *nof* = [2 : 24], hence $\alpha \in [0.1309, 1.5707]$ and $\widetilde{R} \in [0.1, 0.75]$ this would generate an infinite number of choices hence searching for an optimum value where *j* factor is maximum seems to be a gigantic task. Therefore, this necessitates the usage of a numerical optimization technique hence genetic algorithm is employed which searches for the optimum through all the available choices.
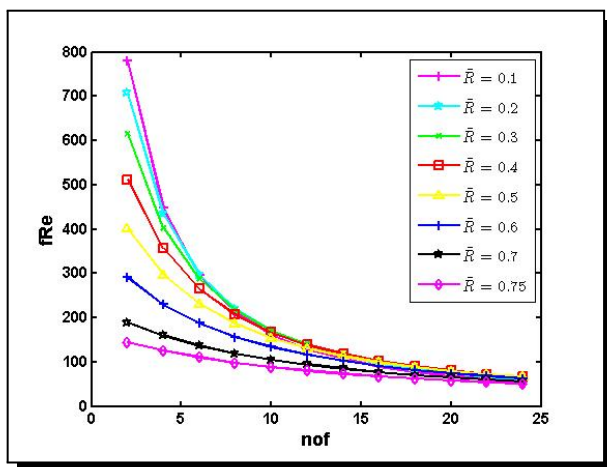


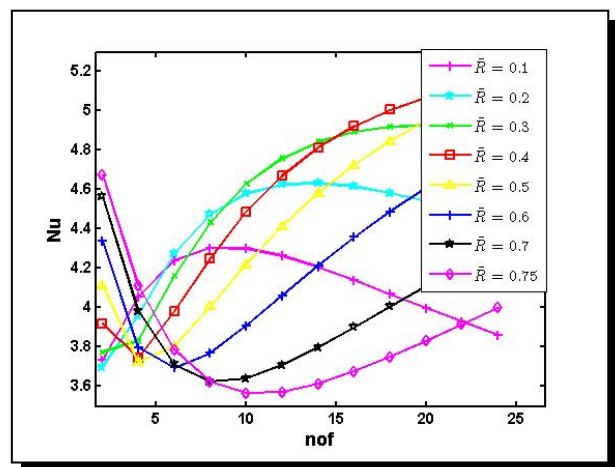**Figure 4.1.** *fRe* for various values of $\widetilde{R}$ while $\widehat{K} = 0.001$

**Figure 4.2.** *Nu* for different values of $\widetilde{R}$ when $\widehat{K} = 0.001$

Our objective is to maximize the heat transfer rate and minimize the friction effect simultaneously, which can prove to be a difficult task. This can be achieved with the help of Colburn's $j$ factor quite easily, which is a correlation between the Nusselt number ($Nu$) and the product of fanning friction and Reynold's number ($fRe$). So it can be observed that Colburn's $j$ factor is a non-dimensional quantity which is an analogy that relates heat transfer coefficients, mass transfer coefficients and friction factor. This relation can be observed in the following equation

$$j \text{ factor} = \frac{NuPr^{\frac{-1}{3}}}{fRe}, \tag{4.1}$$

here $Pr$ is the Prandth number which is a dimensionless quantity that is the ratio between momentum diffusivity to thermal diffusivity. It can be mathematically expressed as [9]

$$Pr = \frac{\mu c_p}{\kappa} = \frac{\upsilon}{\alpha}, \tag{4.2}$$

where $\mu$ represents absolute or dynamic viscosity, $c_p$ is taken as the specific heat capacity and $\kappa$ is used for thermal conductivity. Genetic algorithm maximizes the value of $j$ factor. Hence through Colburn's $j$ factor $Nu$ is being maximized and $fRe$ minimized, this solves our problem of choosing the best desirable result perfectly.

## 4.1 Objective Function

The objective function or fitness function for genetic algorithm is taken as the inverse of Colburn's $j$ factor, which is minimized for ratio of radii and sector angle of channel. Hence by maximizing the $j$ factor we increase the convective heat transfer rate and minimize the friction effect.

## 4.2 Constraints

The prime parameters i.e. ratio of radii $\widetilde{R}$ and the sector angle $\alpha$ (which is shown with the help of number of fins ($nof$)) are bounded by the restrains on their range. For the present optimization process, the range on parameters are taken to be $nof = [2:24]$, hence $\alpha \in [0.1309, 1.5707]$ and $\widetilde{R} \in [0.1, 0.75]$.

## 4.3 Penalty Functions

Genetic algorithms can be directly applied to unconstrained problems. If the need arises to apply GA on constrained problems then the most commonly used method to handle constraints is penalty function. Penalty function transforms constrained to unconstrained problems and then solves them. For more information on penalty function refer to [23].

## 5. Results and Discussion

In this section we will be discussing the results of fluid flow and heat transfer for optimal geometries at Prandtl number 0.707, which is $Pr$ for air. Also a comparison has been made for objective function value when $Pr$ is set to be 7.01, which is $Pr$ for water.

The results of Genetic algorithm, when Prandtl number is fixed at 0.707 and permeability i.e. $\widehat{K} \in [0.001100]$ can be visualized through Figures 5.1 and 5.2. Figure 5.1 is the graphical representation of the best and mean scores of penalty function, through each generation. As our number of fins are bound to be integers and our optimization lies in the category of constrained optimization hence genetic algorithm minimizes penalty function instead of fitness function. Figure 5.1 exhibit the behavior of inverse of $j$ factor i.e. $\frac{1}{j \text{ factor}}$ by its best and mean values versus generations. It can be seen, an individual plot, that in the initial generations the best and mean penalty values are far apart but rapidly the maximum value declines and comes almost in line with the mean score values until the algorithm converges, the stopping criteria is met and generations of objective function stop. This shows that genetic algorithm is working by decreasing the value of fitness function through each generation. Also as the permeability of porous medium, $\widehat{K}$ increases shown in Figures 5.1a-5.1f the best penalty value decreases. This occurs due to the more available space for fluid flow hence friction effect and convective heat transfer decrease but the decrease in friction is more prominent than heat transfer hence this results in a decline in objective function value.

Figure 5.2 portrays the minimum, maximum and the average values of fitness function in each generation, it is recognized as the range plot. Figures 5.2a-5.2f describe effect of permeability $\widehat{K}$ on the fitness function through generations. Also, it can be observed that best, worst and mean scores of objective function come close to each other with each passing generation as genetic algorithm converges. It can be seen through each sub-figure in Figure 5.2 that with the decreases in $\widehat{K}$ the objective function escalates as there are more high peaked objective function generations. Also with the falling value of $\widehat{K}$ the free available space for fluid flow decreases hence the friction effect represented by *fRe* and heat transfer recognized through *Nu* increases but the upsurge in *fRe* is more than *Nu* so objective function experiences an boost in its value.

Table 5.1 demonstrates the influence of permeability on the optimum geometry exhibited by geometric components such as ratio of radii $\widetilde{R}$ and number of fins (*nof*) where the Prandtl number is fixed to be 0.707. The corresponding optimum values of *Nu* and *fRe* are also given for each value of permeability in porous media, along with the maximum value of objective function (*j* factor), where *nof* is bounded as: $nof = [2 : 24]$, $\alpha \in [0.1309, 1.5707]$ and $\widetilde{R} \in [0.2, 0.75]$. Table shows that with the decrease in permeability of porous media the value of objective function gradually declines, whereas *fRe* and *Nu* increases but the upsurge in *fRe* is more notable than the increase in *Nu*. As *j* factor is a correlation between *Nu* and *fRe* then this behavior of *Nu* and *fRe* decreases the value of *j* factor. The changes in *fRe* and *Nu* arises due to the high dependence of friction factor and Nusselt number on the conduct of ratio of radii, number of fins and permeability.

It can be observed that with the decrease in $\widehat{K}$, the optimum or best value of $\widetilde{R}$ experiences a slow decrease in its value whereas *nof* is constant at maximum value of fins. So due to less free space, as both $\widetilde{R}$ and permeability of porous media are small *fRe* becomes large but it is still the least, most feasible amount for a particular value of permeability. *Nu* experiences slight fluctuations which are very minuscule but on the whole it increases. This slight elevation in the

value of $Nu$ can be due to porous media, as permeability decreases the porous media becomes more packed hence helps increase the rate of heat conduction. The optimum value of number of fins is seen to be at its maximum value because as the fins are taken to be highly conductive then greater the amount of heat conducting surface more will be the rate of convective heat transfer. With the decreases in $\widehat{K}$, the optimum value of $\widetilde{R}$ experiences a minute decreases hence more space is available for fluid flow which creates a balance with the low permeability, so that the desired surge in $Nu$ is achieved. It is noted that optimal value of ratio of radii $\widetilde{R}$ at each value of $\widehat{K}$, is found almost midway in the range set for $\widetilde{R}$ i.e. $\widetilde{R} \in [0.1, 0.75]$. This behavior indicates that optimum value does not occur when $\widetilde{R}$ is too small because for smaller $\widetilde{R}$, $fRe$ raises which is not our desired outcome. Genetic algorithm looks past the maximum value in range of $\widetilde{R}$ for optimum because although friction effect decreases so does the convection rate due to large distance between conductive surfaces. Hence a middle value gives optimum.

**Table 5.1.** Effect of permeability on optimal geometric parameters

| $\widehat{K}$ | Geometric Components | | $j$ factor | $fRe$ | $Nu$ |
| | $\widetilde{R}$ | $nof$ | | | |
|---|---|---|---|---|---|
| 100 | 0.570127758897386 | 24 | 0.308111604235642 | 15.605687585626500 | 4.283486819490765 |
| 10 | 0.570115335784497 | 24 | 0.308026794022231 | 15.610494379960882 | 4.283626772414494 |
| 1 | 0.569991181369073 | 24 | 0.307181547770969 | 15.658558525894634 | 4.285025151868879 |
| 0.1 | 0.568709076515744 | 24 | 0.299005429710323 | 16.139216984288254 | 4.299005558385511 |
| 0.01 | 0.553392324178606 | 24 | 0.237719484798629 | 20.944235305204661 | 4.435430311389410 |
| 0.001 | 0.416706766714202 | 24 | 0.088042418303868 | 65.787935927488192 | 5.159940515716588 |

We exhibit in Table 5.2, the impact of various permeabilities on objective function where a comparison is done for the value of Prandtl number taken to be 7.01, which is $Pr$ for water at 20 degree centigrade and $Pr = 0.707$. The table shows that, with the decrease in permeability of porous media, for both values of Prandtl number, $j$ factor shows a steady decline. This occurs due to the co-dependence of $j$ factor on $fRe$ and $Nu$. $fRe$ and $Nu$ increases with the decrease in $\widehat{K}$ but the upsurge in $fRe$ is more notable than the increase in $Nu$. The value of $j$ factor for $Pr = 0.707$ is more then that of $Pr = 7.01$ at every $\widehat{K}$ because when $Pr$ is small thermal divisibility is more than kinematic viscosity (refer to formula (4.2)) hence to increase heat transfer rate $Pr$ should be kept small so at $Pr = 0.707$, $j$ factor shows greater values than for $Pr = 7.01$ as $j$ factor is ratio of $Nu$ to the product of $fRe$ and a power of $Pr$.

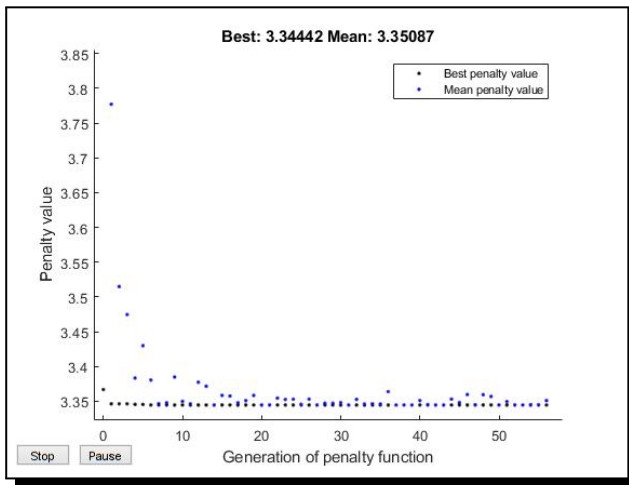**Table 5.2.** A comparison of optimal objective function value for $Pr = 0.707$ and $Pr = 7.01$

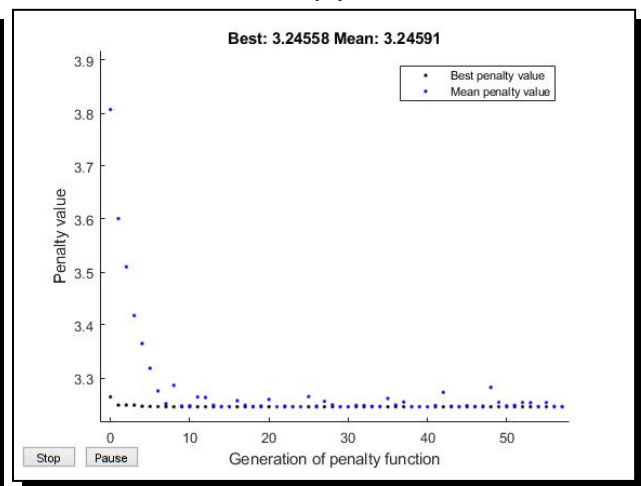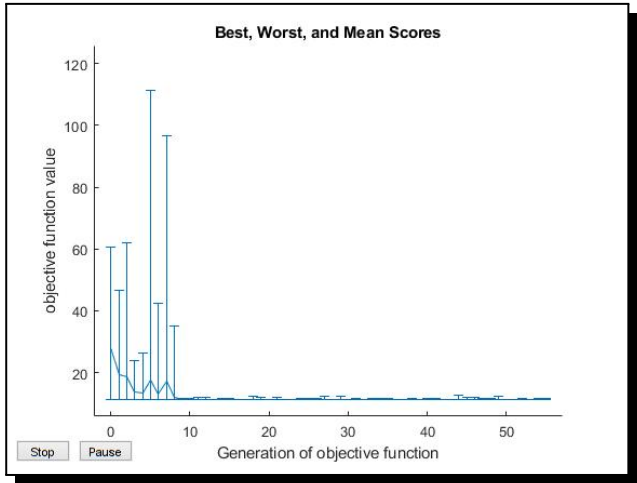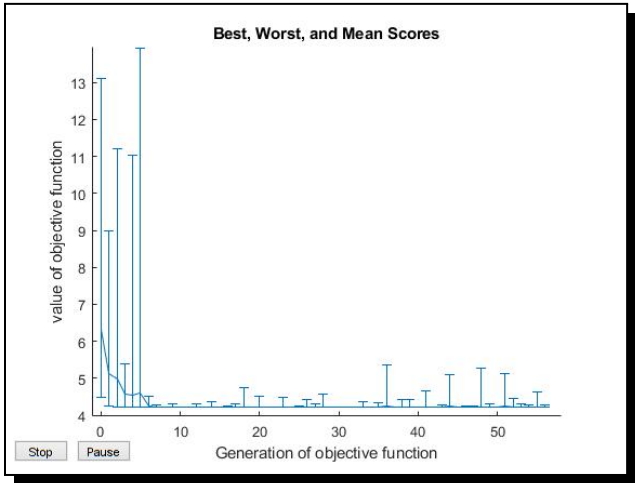| $\widehat{K}$ | $Pr = 0.707$ | $Pr = 7.01$ |
| | $j$ factor value | |
|---|---|---|
| 100 | 0.308111604235642 | 0.143419604484919 |
| 10 | 0.308026794022231 | 0.143380127077719 |
| 1 | 0.307181547770969 | 0.142986682360343 |
| 0.1 | 0.299005429710323 | 0.139180867836127 |
| 0.01 | 0.237719484798629 | 0.110653523007539 |
| 0.001 | 0.088042418303868 | 0.040981931992991 |
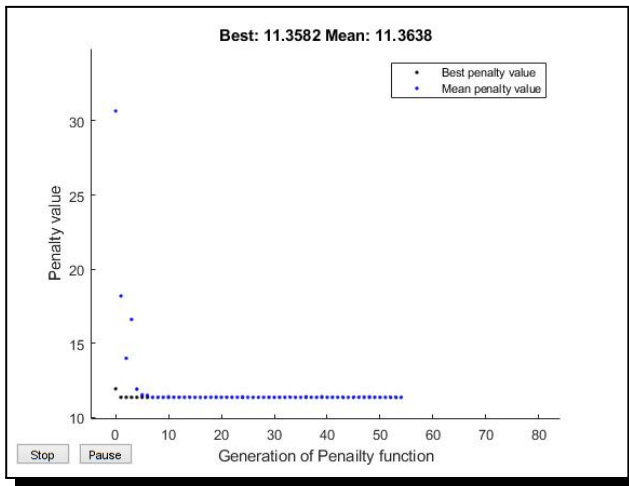
**(a)**
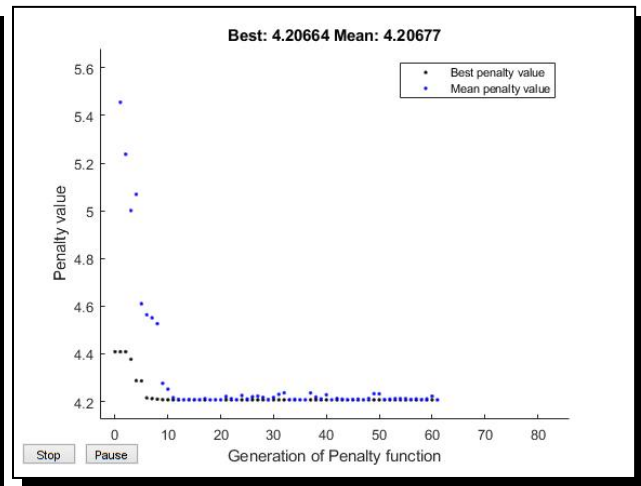
**(b)**

**(c)**
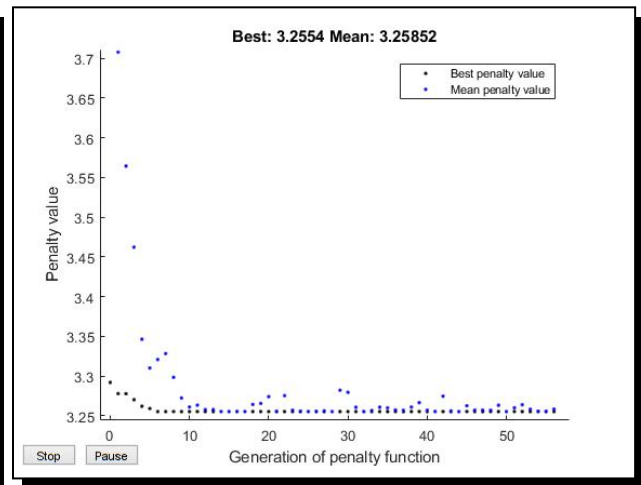
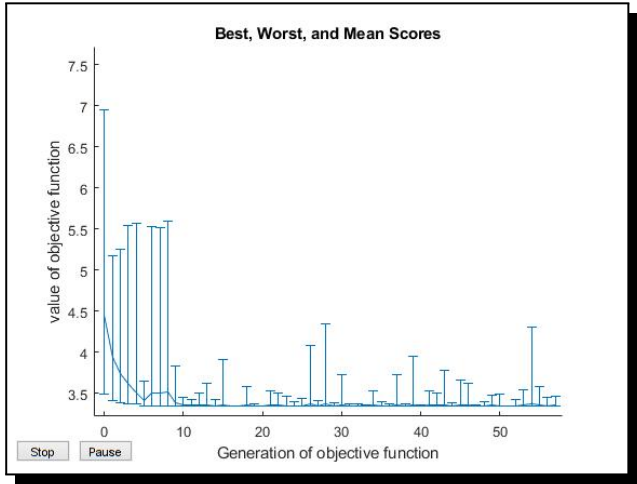**(d)**
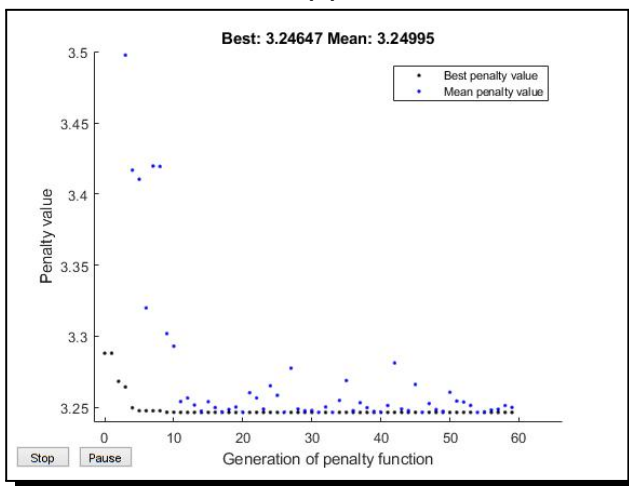
**(e)**

**(f)**

**Figure 5.1.** Best fitness plot at $Pr = 0.707$ for (a): $\widehat{K} = 0.001$  (b): $\widehat{K} = 0.01$  (c): $\widehat{K} = 0.1$  (d): $\widehat{K} = 1$ (e): $\widehat{K} = 10$  (f): $\widehat{K} = 100$
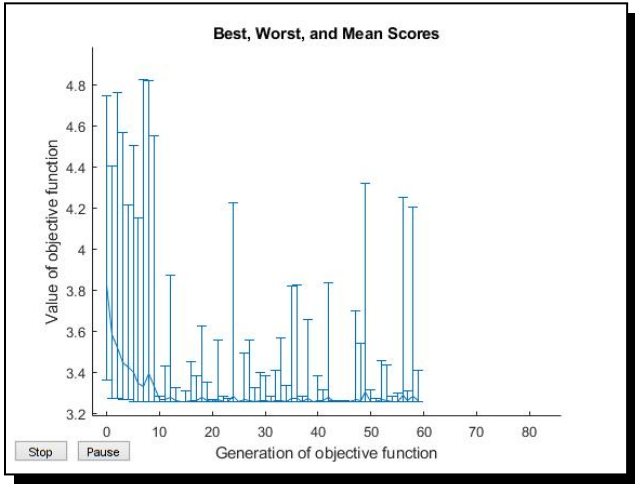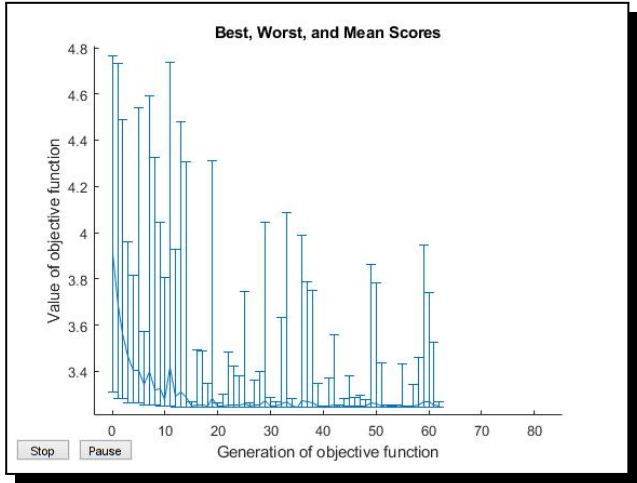
**(a)**

**(b)**

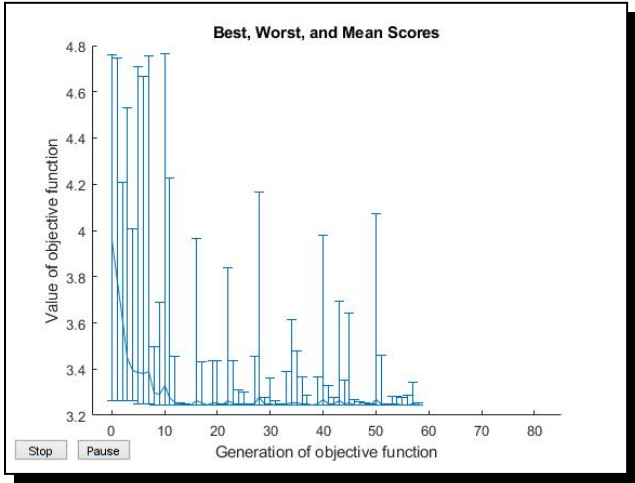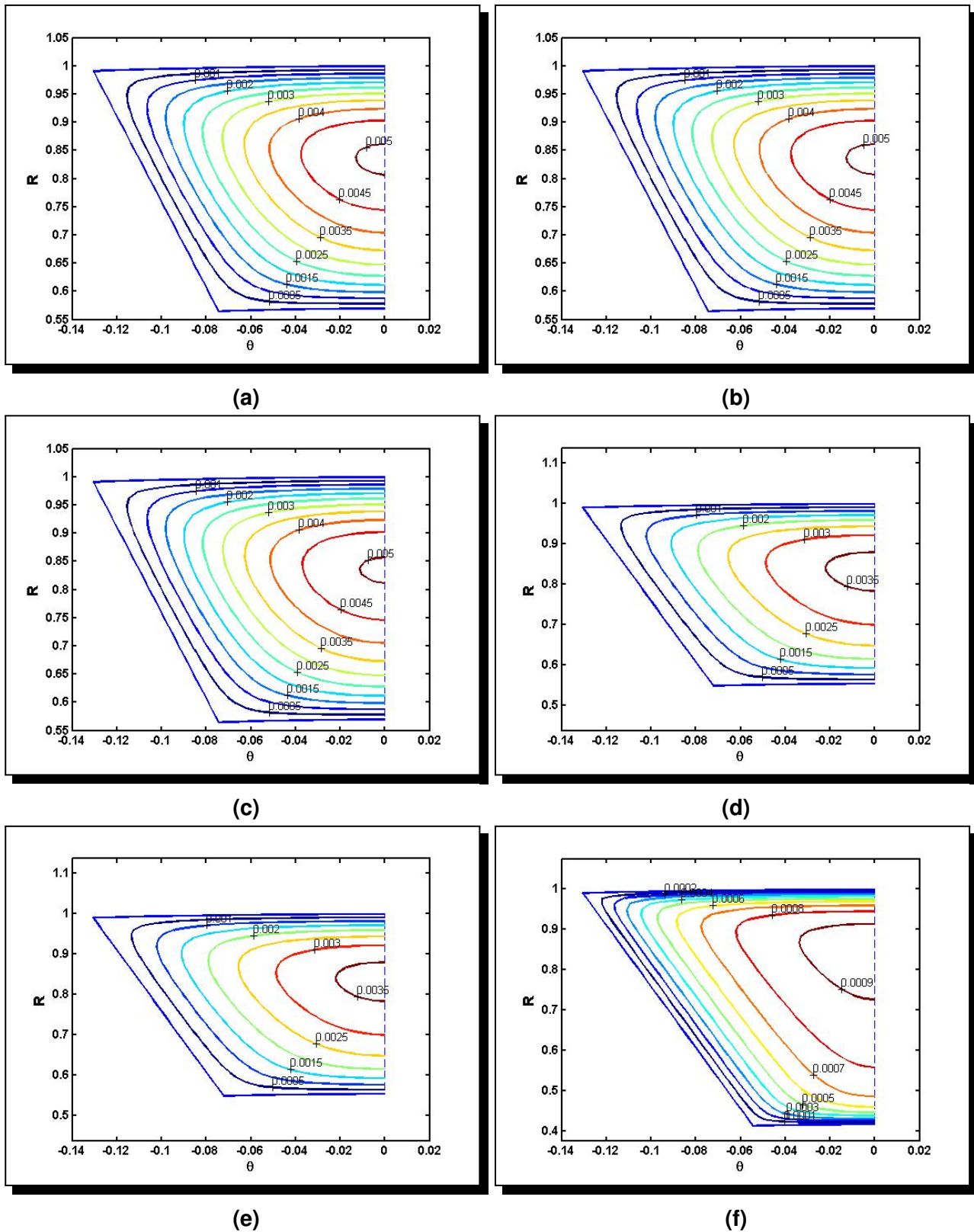**(c)**

**(d)**

**(e)**

**(f)**

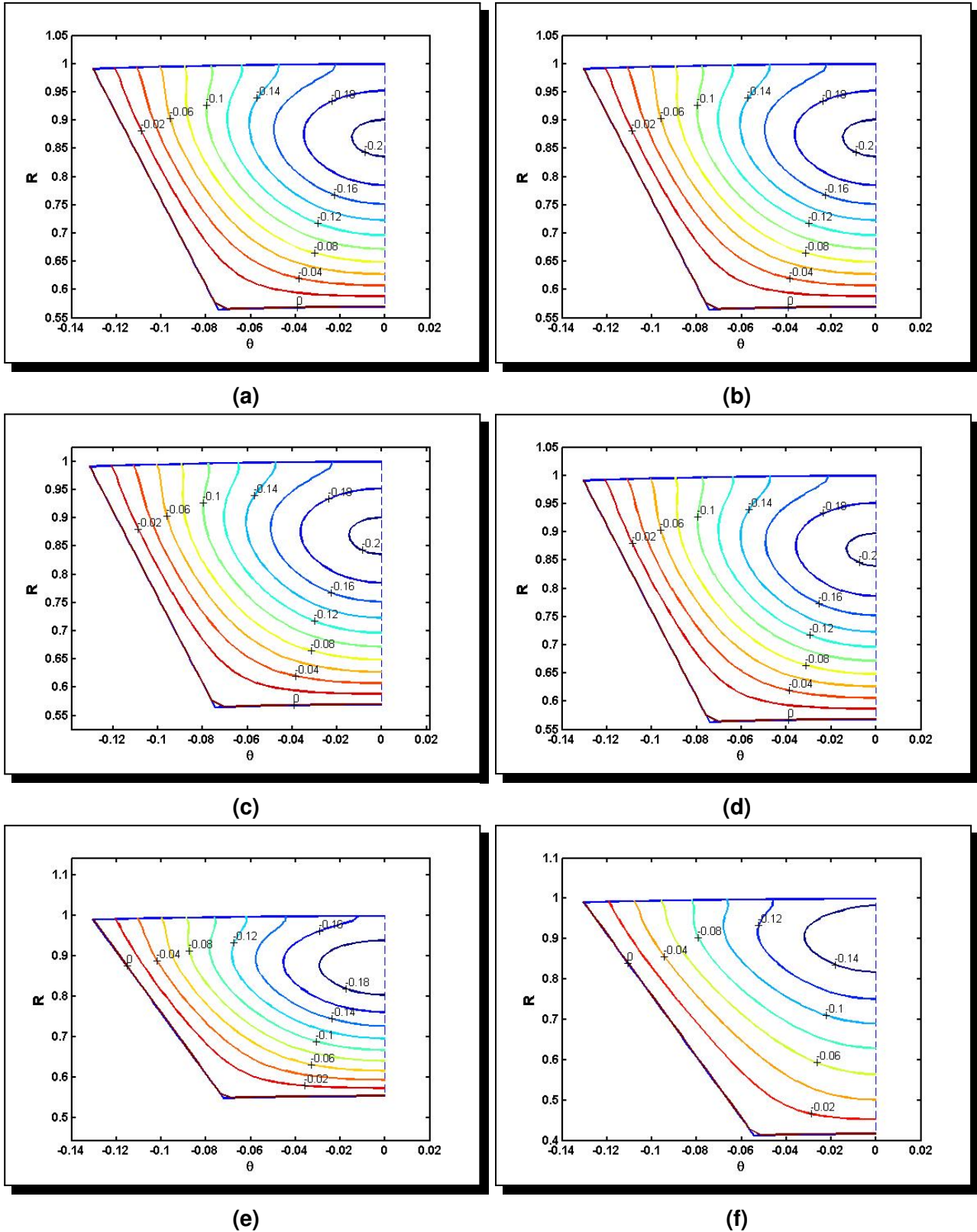**Figure 5.2.** Range plot at $Pr = 0.707$ for (a): $\widehat{K} = 0.001$  (b): $\widehat{K} = 0.01$  (c): $\widehat{K} = 0.1$  (d): $\widehat{K} = 1$  (e): $\widehat{K} = 10$ (f): $\widehat{K} = 100$

**Figure 5.3.** Velocity profile at $Pr = 0.707$ for (a):$\widehat{K} = 100$ (b): $\widehat{K} = 10$ (c): $\widehat{K} = 1$ (d): $\widehat{K} = 0.1$ (e): $\widehat{K} = 0.01$ (f): $\widehat{K} = 0.001$

(a)



(b)



(c)



(d)



(e)



(f)

**Figure 5.4.** Temperature profile at $Pr = 0.707$ for (a): $\widehat{K} = 100$ (b): $\widehat{K} = 10$ (c): $\widehat{K} = 1$ (d): $\widehat{K} = 0.1$ (e): $\widehat{K} = 0.01$ (f): $\widehat{K} = 0.001$

Now the impact created by various permeabilities over the optimum velocity profile would be analyzed, where $\hat{K} \in [0.001100]$. Figure 5.3 show the velocity contours for the optimal value of $\widetilde{R}$ and $\alpha$. After examining Figures 5.3a–5.3f an increase in the velocity gradients among adjacent layers in the fluid as $\hat{K}$ declines can be observed. This is the reason behind the decrease in bulk velocity and increases the *fRe* with decreasing permeability. As the permeability falls the maximum velocity region grows.

Figures 5.4 exhibit the isotherms for optimal value of $\widetilde{R}$ and $\alpha$ at each $\hat{K}$. Figures 5.4a–5.4f demonstrate the influence created by decreasing the permeability on the temperature profile. Through the impressions of sub-figures a temperature difference from the heated surfaces can be observed, heated surfaces being the wall of inner pipe and the fin surface. Through Figures 5.4a-(5.4f it can be detected that, with the decline in permeability heat transfer increases gradually as the temperature difference among heated wall and the fluid grows at a certain point.

## 6. Conclusion

In this research, the optimization of an annulus sector duct filled with Darcy-Brinkman's porous media has been conducted. The desired optimization outcome is approached by employing *Genetic Algorithm* (GA). We optimized duct geometry i.e. number of fins and ratio of radii while setting *j* factor as the objective function. It can be concluded, from the results observed in this study, that with the decrease in permeability the optimum values of *fRe* and *Nu* both exhibit an increase. Also the optimal sector angle is its upper bound value and it remains consistent for all permeabilities.

### Competing Interests

The authors declare that they have no competing interests.

### Authors' Contributions

All the authors contributed significantly in writing this article. The authors read and approved the final manuscript.

## References

[1] I.K. Adegun, T.S. Jolayemi, O.A. Olayemi and A.M. Adebisi, Numerical simulation of forced convection heat transfer in inclined elliptical ducts with multiple internal longitudinal fins, *Alexandria Engineering Journal* (2017), DOI: 10.1016/j.aej.2017.01.014.

[2] J.D. Anderson, Jr., *Computational Fluid Dynamics*, McGraw Hill (1995).

[3] S. Colle and C.R. Maliska, Optimization of finned double tubes for heat transfer in laminar flow, *Brazilian Congress on Mechanical Engineering, Rio de Janeiro, Universidade Fedural, B* (1976), 475 – 490.

[4] A.R. Conn, N.I.M. Gould and Ph. L. Toint, Trust-region methods, *MPS-SIAM Series on Optimization*, SIAM, Philadelphia (2000).

[5] G. Fabbri, A genetic algorithm for fin profile optimization, International *Journal of Heat and Mass Transfer* **40** (9) (1997), 2165 – 2172, DOI: 10.1016/S0017-9310(96)00294-3.

**[6]** C.J. Geankoplis, *Transport Processes and Separation Process Principles (includes Unit Operations)*, 4th edition, (2003), 475.

**[7]** S. Gosselin, Review of utilization of genetic algorithms in heat transfer problems, *International Journal of Heat and Mass Transfer* **52** (2009), 2169 – 2188, DOI: 10.1016/j.ijheatmasstransfer.2008.11.015.

**[8]** K. Hooman, H. Gurgenci and A.A. Merrikh, Heat transfer and entropy generation optimization of forced convection in porous-saturated ducts of rectangular cross-section, *International Journal of Heat and Mass Transfer* **50** (2007) 2051 – 2059, DOI: 10.1016/j.ijheatmasstransfer.2006.11.015.

**[9]** F.P. Incropera, D.P. DeWitt, T. Bergman and A. Lavine, *Fundamentals of Heat and Mass Transfer*, J. Wiley, 6 (2007).

**[10]** M. Iqbal and H. Afaq, Fluid flow and heat transfer through an annular sector duct filled with porous media, *Journal of Porous Media* **18** (7) (2015), 679 – 687, DOI: 10.1615/JPorMedia.v18.i7.30.

**[11]** Z. Iqbal, K.S. Syed and M. Ishaq, Optimal configuration of finned annulus in a double pipe with fully developed laminar flow, *Applied Thermal Engineering* **31** (2011) 1435 – 1446, DOI: 10.1016/j.applthermaleng.2011.01.012.

**[12]** Z. Iqbal, K.S. Syed and M. Ishaq, Optimal convective heat transfer in double pipe with parabolic fins, *International Journal of Heat and Mass Transfer* **54** (2011), 5415 – 5426, DOI: 10.1016/j.ijheatmasstransfer.2011.08.001.

**[13]** Z. Iqbal, K.S. Syed and M. Ishaq, Fin design for conjugate heat transfer optimization in double pipe, *International Journal of Thermal Sciences* **94** (2015), 242 – 258. DOI: 10.1016.2Fj.ijthermalsci.2015.03.011.

**[14]** Z. Iqbal, K.S. Syed and M. Ishaq, Optimal fin shape in finned double pipe with fully developed laminar flow, *Applied Thermal Engineering* **51** (2013), 1202 – 1223.

**[15]** M. Ishaq, K.S. Syed, Z. Iqbal, A. Hassan and A. Ali, DG-FEM based simulation of laminar convection in an annulus with triangular fins of different heights, *International Journal of Thermal Sciences* **72** (2013), 125 – 146, DOI: 10.1016/j.ijthermalsci.2013.04.022.

**[16]** M. Kaviany, Laminar flow through a porous channel bounded by isothermal parallel plates, *International Journal Heat Mass Transfer* **28** (4) (1985), 851 – 858, DOI: 10.1016/0017-9310(85)90234-0.

**[17]** I. Kurtbas and N. Celik, Experimental investigation of forced and mixed convection heat transfer in a foam filled horizontal rectangular channel, *International Journal of Heat and Mass Transfer* **52** (2009), 1313 – 1325, DOI: 10.1016/j.ijheatmasstransfer.2008.07.050.

**[18]** Z.Y. Li, T.C. Hung and W.Q. Tao, Numerical simulation of fully developed turbulent flow and heat transfer in annular-sector ducts, *Heat and Mass Transfer* **38** (4-5) (2002), 369 – 377, DOI: 10.1007/s002310100224.

**[19]** M.J. Lin, Q.W. Wang and W.Q. Tao, Developing laminar flow and heat transfer in annular-sector ducts, *Heat Transfer Engineering* **21**(2) (2000) 53 – 61, DOI: 10.1080/014576300271022.

**[20]** F. Liu, The effect of geometries on heat transfer enhancement of thermal fluids in curved ducts, *Applied Thermal Engineering* **90** (2015), 590 – 595, DOI: 10.1016%2Fj.applthermaleng.2015.07.046.

**[21]** J.M. McDonough, *Lectures in Elementary Fluid Dynamics*, (2009), `http://web.engr.uky.edu/~acfd/me330-lctrs.pdf`.

**[22]** M.R.H. Nobari and M.T. Mehrabani, A numerical study of fluid flow and heat transfer in eccentric curved annuli, *International Journal of Thermal Sciences* **49** (2010), 380 – 396, DOI: 10.1016/j.ijthermalsci.2009.07.003.

**[23]** Ö. Yeniay, Penalty function methods for constrained optimization with genetic algorithms, *Mathematical and Computational Applications* **10** (1) (2005), 45 – 56, DOI: 10.3390/mca10010045.

**[24]** R.K. Shah and A.L. London, *Laminar Flow Forced Convection in Ducts*, Academic Press, London (1978).

**[25]** H.J. Sung, S.Y. Kim and J.M. Hyun, Forced convection from an isolated heat source in a channel with porous medium, *International Journal Heat and Fluid Flow* **16** (1995), 527 – 535, DOI: 10.1016/0142-727X(95)00032-L.

**[26]** Y.X. Yauan, A review of trust region algorithms for optimization, J.M. Ball and J.C.R. Hunt (eds.), *Proceedings of the Fourth International Congress on Industrial and Applied Mathematics*, Oxford University Press (2000), 271 – 282.

**[27]** E.H. Zaim and S.A.G. Nassab, Numerical investigation of laminar forced convection of water upwards in a narrow annulus at supercritical pressure, *Energy* **35** (10) (2010), 4172 – 4177, `https://www.cheric.org/research/tech/periodicals/doi.php?art_seq=859872`.

**[28]** O. Zeitoun and A.S. Hegazy, Heat transfer for laminar flow in internally finned pipes with different fin heights and uniform wall temperature, *Heat Mass Transfer* **40** (2004), 253 – 259, DOI: 10.1007/s00231-003-0446-8.